# A Meiotic Drive Element in the Maize Pathogen *Fusarium verticillioides* Is Located Within a 102 kb Region of Chromosome V

**Jay Pyle,* Tejas Patel,* Brianna Merrill,* Chabu Nsokoshi,* Morgan McCall,* Robert H. Proctor,† Daren W. Brown,†,1 and Thomas M. Hammond*,1**

*School of Biological Sciences, Illinois State University, Normal, Illinois 61790, and †Mycotoxin Prevention and Applied Microbiology, National Center for Agricultural Utilization Research, U.S. Department of Agriculture, Agricultural Research Service, Peoria, Illinois 61604

**ABSTRACT** *Fusarium verticillioides* is an agriculturally important fungus because of its association with maize and its propensity to contaminate grain with toxic compounds. Some isolates of the fungus harbor a meiotic drive element known as *Spore killer* ($Sk^K$) that causes nearly all surviving meiotic progeny from an $Sk^K \times$ *Spore killer*-susceptible ($Sk^S$) cross to inherit the $Sk^K$ allele. $Sk^K$ has been mapped to chromosome V but the genetic element responsible for meiotic drive has yet to be identified. In this study, we used cleaved amplified polymorphic sequence markers to genotype individual progeny from an $Sk^K \times Sk^S$ mapping population. We also sequenced the genomes of three progeny from the mapping population to determine their single nucleotide polymorphisms. These techniques allowed us to refine the location of $Sk^K$ to a contiguous 102 kb interval of chromosome V, herein referred to as the *Sk* region. Relative to $Sk^S$ genotypes, $Sk^K$ genotypes have one extra gene within this region for a total of 42 genes. The additional gene in $Sk^K$ genotypes, herein named *SKC1* for *Spore Killer Candidate 1*, is the most highly expressed gene from the *Sk* region during early stages of sexual development. The *Sk* region also has three hyper-variable regions, the longest of which includes *SKC1*. The possibility that *SKC1*, or another gene from the *Sk* region, is an essential component of meiotic drive and spore killing is discussed.

**KEYWORDS**
genomic conflict
mapping
meiotic drive
fungi
spore killing

*Fusarium verticillioides* is an ascomycete fungus that can exhibit both endophytic and pathogenic growth on maize (Bacon and Hinton 1996; White 1998). The fungus is of agricultural concern because of its ability to cause maize ear and stalk rot and also because it can contaminate maize kernels with a group of mycotoxins known as fumonisins (Marasas 2001; (Munkvold and Desjardins 1997). The problems caused by *F. verticillioides* and its myoctoxins were noticed as early as 1970, when the fungus was correlated with an outbreak of equine leukoencephalomalacia (ELEM) in South Africa (Kellerman *et al.* 1972). Since then, fumonisins have been confirmed to cause ELEM in horses (Marasas *et al.* 1988; Kellerman *et al.* 1990), pulmonary edema in pigs (Harrison *et al.* 1990), and liver cancer in laboratory rats (Gelderblom *et al.* 1988, 1991). Fumonisin-contaminated grain has also been linked to neural tube defects in humans (Missmer *et al.* 2006). Thus, the potential presence of fumonisins, even in apparently healthy grain, makes it necessary to aggressively screen grain for these mycotoxins. Contaminated grain must be destroyed, resulting in crop losses worth millions of dollars per yr (Wu 2007).

The primary sources of inoculum for endophytic and pathogenic growth of *F. verticillioides* on maize are asexual spores known as macroconidia and microconidia (Munkvold 2003). Sexual spores, called ascospores, may also be important to the *F. verticillioides* life cycle (Reynoso *et al.* 2009). Sexual reproduction in this heterothallic fungus begins when the immature fruiting bodies of one strain are fertilized by a strain of opposite mating type (Martin *et al.* 2011). Fruiting bodies are called perithecia and meiosis occurs in spore sacs, called asci, within the perithecia. At the start of meiosis, a single diploid nucleus is formed


doi: 10.1534/g3.116.029728
Manuscript received March 26, 2016; accepted for publication June 6, 2016; published Early Online June 10, 2016.

Supplemental material is available online at www.g3journal.org/lookup/suppl/doi:10.1534/g3.116.029728/-/DC1
[1]Corresponding authors: National Center for Agricultural Utilization Research 1815 N University St., Peoria, IL 61604. E-mail: daren.brown@ars.usda.gov; and Illinois State University, School of Biological Sciences, Julian Hall 210, Campus Box 4120, Normal, IL 61790. E-mail: tmhammo@ilstu.edu

**Table 1 Key strains used in this study**

| Name[a] | Genotype | Alternate Names |
|---|---|---|
| Fv149 | *Sk*$^S$, *MAT-1* | FGSC 7600,[b] M-3125,[c] A00149[c] |
| Fv999 | *Sk*$^K$, *MAT-2* | FGSC 7603,[b] A00999[d] |
| RJP98.75 | *Sk*$^K$, *MAT-2* | This study |
| RJP98.111 | *Sk*$^K$, *MAT-2* | This study |
| RJP98.118 | *Sk*$^K$, *MAT-2* | This study |
| RBM43.31 | *Sk*$^K$, *MAT-1* | This study |

[a] Throughout the text, the suffix -*Sk*$^K$ or -*Sk*$^S$ is added to each strain name to denote genotype with respect to *Sk*.
[b] McCluskey *et al.* 2010.
[c] Xu *et al.* 1995.
[d] Xu and Leslie 1996.

from the haploid genomes of both parents. This diploid nucleus separates into four haploid nuclei through the standard reductional and equational division stages of meiosis, and each of the four haploid nuclei undergoes a postmeiotic mitosis to form eight nuclei. Each nucleus is then incorporated into an ascospore through a process known as ascospore delimitation. A phenotypically normal ascus should thus contain eight ascospores at maturity in *F. verticillioides*.

During normal development, asci break down and ascospores are exuded from perithecia in gelatinous masses. It is possible, however, to examine ascospores within intact asci by perithecial dissection. Kathariou and Spieth (1982) used this technique during their discovery of an allele named *Spore killer* (*Sk*$^K$). In *Sk*$^K$ × *Sk*$^S$ crosses, where the latter stands for *Spore killer*-susceptible, asci contain four instead of eight ascospores (Kathariou and Spieth 1982). While early stages of ascus development are cytologically normal in these crosses, four ascospores degenerate shortly after ascospore delimitation (Raju 1994). The four surviving ascospores are almost always of the *Sk*$^K$ genotype (Kathariou and Spieth 1982; Xu and Leslie 1996). Unlike *Sk*$^K$ × *Sk*$^S$ crosses, *Sk*$^K$ × *Sk*$^K$ crosses produce asci with eight ascospores (Kathariou and Spieth 1982). The *Sk*$^K$ allele is thus sufficient for both spore killing and resistance to killing.

The ability of *Sk*$^K$-ascospores to kill *Sk*$^S$-ascospores suggests that *Sk*$^K$ could be the predominant allele in some *F. verticillioides* populations. Although the literature is limited on this subject, a screen of 225 *F. verticillioides* isolates from 24 fields across Europe and North America found the *Sk*$^K$ allele to be present in 81% of isolates (Kathariou and Spieth 1982). Shortly after the discovery of *Sk*$^K$ in *F. verticillioides*, a spore killing allele was also discovered in *F. subglutinans* (Sidhu 1984). While this allele was also named *Spore killer*, it was given the slightly different notation of *SK*$^k$. Sidhu (1984) presented evidence that *SK*$^k$ was present in 10 of 15 *F. subglutinans* isolates obtained from a single maize field. Therefore, *Sk*$^K$ and *SK*$^k$ appear to be the predominant alleles in at least some populations of *F. verticillioides* and *F. subglutinans*.

The relationship between *Sk*$^K$ and *SK*$^k$ is still unclear. To our knowledge, the only other significant research involving either allele was performed by Xu and Leslie (1996) during construction of an *F. verticillioides* genetic map. During this study, *Sk*$^K$ was mapped between two restriction fragment length polymorphism (RFLP) markers on chromosome V. These markers, named RFLP1 and 11p18, are located 2.5 cM and 8.6 cM from *Sk*$^K$, respectively (Xu and Leslie 1996). Xu and Leslie's mapping population was derived from an *Sk*$^K$ × *Sk*$^S$ cross, and, interestingly, only one of more than 100 progeny did not inherit the *Sk*$^K$ allele (Xu and Leslie 1996), demonstrating that *Sk*$^K$ can achieve transmission rates of over 99% in laboratory crosses.

An *F. verticillioides* reference genome, derived from an *Sk*$^S$ strain known as Fv149-*Sk*$^S$, was published 14 yr after the initial mapping of *Sk*$^K$ (Ma *et al.* 2010). Here, we advance *Fusarium* Spore killer research by delineating physical borders for *Sk*$^K$ with respect to this reference genome. Our data place *Sk*$^K$ within a 102 kb contiguous sequence of DNA, which we refer to as the *Sk* region. Notable differences exist between this region in the *Sk*$^K$ and *Sk*$^S$ strains examined in this study. These are described and discussed below.

## MATERIALS AND METHODS

### Strains, media, and culture conditions

Key strains are listed in Table 1. Vegetative propagation was performed on V8 juice agar (VJA) (Tuite 1969) in 16 mm test tubes at room temperature on a laboratory benchtop. Carrot agar (CA), which was originally described by Klittich and Leslie (1988), was prepared as follows: 200 g of organic peeled baby cut carrots were autoclaved in 200 ml of water, pureed with a blender, then adjusted to 500 ml with sterile water to create a 1× stock. Diluted CA (*e.g.*, 0.1× and 0.25×) was prepared by mixing the appropriate volumes of 1× CA stock and sterile water before adding agar to a final concentration of 2% and autoclaving. Liquid Vogel's Minimal medium (VMM, Vogel 1956) or GYP medium (2% glucose, 1% peptone, and 0.3% yeast extract) were used to produce mycelia for genomic DNA isolation. Liquid cultures for genomic DNA isolation were incubated at 28° in the dark without agitation.

### Sexual crosses

Crosses were performed on CA in a manner similar to previously described methods (Klittich and Leslie 1988). Asexual spores (conidia) from the female parent were transferred to the center of a 60 mm petri dish containing 20 ml of CA or diluted CA. The female parent was then cultured for 10−14 d before fertilization with a suspension of conidia from the male parent. Conidial suspensions were prepared by adding 2.0 ml of 0.001% Tween-20 to a 10- to 14-d-old test-tube culture of the male parent and dislodging the conidia with a pipette tip. Fertilization was performed by transferring 1.0 ml of this conidial suspension to the surface of a culture of the female parent. The conidial suspension was spread over the surface of the female culture with a glass rod. Crosses were incubated in a culture chamber that alternated between 23.0°

**Table 2 Draft genome assembly statistics**

| Name | Total[a] | Contigs | Avg. Length[b] | # Reads | N50 | Coverage[c] |
|---|---|---|---|---|---|---|
| Fv999-*Sk*$^K$ | 41,922,529 | 855 | 255 | 10,956,620 | 109,413 | 67 |
| RPJ98.75-*Sk*$^K$ | 41,848,894 | 985 | 257 | 8,087,199 | 91,461 | 50 |
| RPJ98.111-*Sk*$^K$ | 41,892,017 | 841 | 242 | 12,538,869 | 120,565 | 72 |
| RPJ98.118-*Sk*$^K$ | 41,868,129 | 914 | 268 | 9,009,572 | 88,867 | 58 |

[a] Total, the total length of each genome assembly.
[b] Avg. length, the average length of each read in the assembly.
[c] Coverage, calculated by multiplying the number of reads by the average read length and dividing the product by 41.9 Mb, the genome size of Fv149-*Sk*$^S$ (NCBI ASM14955v1).

**Table 3 Marker locations**

| Marker[a] | Chromosome | Position (Mb) |
|---|---|---|
| CAPS-1 | V | 1.47 |
| CAPS-2 | V | 1.42 |
| CAPS-3 | V | 0.78 |
| CAPS-4 | V | 0.43 |
| CAPS-5 | V | 0.02 |
| CAPS-6 | V | 2.12 |
| CAPS-9 | XI | 0.07 |
| CAPS-10 | VII | 1.05 |
| CAPS-11 | I | 0.73 |
| RFLP-11p18 | V | 1.67 |

[a] Marker locations on chromosomes I, V, VII, and XI of *F. verticillioides* Fv149-$Sk^S$ (NCBI ASM14955v1).

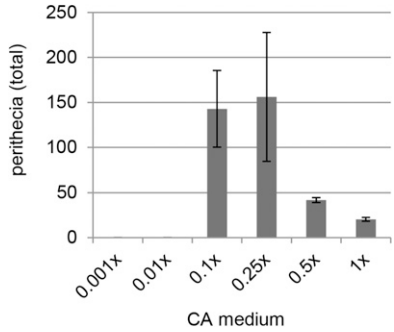


**Figure 1** Perithecial production on different concentrations of carrot in CA medium. Cultures of Fv999-$Sk^K$ were grown on CA containing different concentrations of carrot and fertilized with conidia from strain Fv149-$Sk^S$. The data represent the total number of perithecia observed 25 d after fertilization. Crosses were performed in triplicate. Error bars are standard deviation.

(12 hr, light) and 22.5° (12 hr, dark). Light was provided by white (Philips F34T12/CW/RS/EW/ALTO) and black (General Electric F40T12BL) fluorescent lamps.

### The Fv999-$Sk^K$ × Fv149-$Sk^S$ mapping population

In *F. verticillioides*, ascospores are exuded from mature perithecia in a hair-like structure called a cirrus. To obtain an $Sk^K$ mapping population, Fv999-$Sk^K$ was crossed with Fv149-$Sk^S$ and cirri were isolated from the tops of a few perithecia with a sterile needle, dispersed in sterile water, and spread onto a plate of 4% water agar. Germinating ascospores were transferred to VJA in 16 mm test tubes.

### Microscopy

Asci were dissected from perithecia in 25% glycerol under magnification. A Vanguard 1433Phi light microscope and attached digital camera (Amscope MU1000) were used for imaging. The condenser and aperture diaphragm were set for high contrast, which allowed for the number of ascospores in mature asci to be determined without tissue staining.

### DNA methods

Genomic DNA was prepared using one of three methods. In method one, strains were cultured in 25 ml liquid VMM at 28° in the dark for 3 d. Mycelia were washed with 0.9% NaCl and dried by lyophilization before extraction with IBI Scientific's Genomic DNA Mini Kit for Plants. Method two, based on Henderson *et al.* (2005), was used as an inexpensive and time-efficient alternative to method one. A 6-inch plain-tipped wood applicator was used to transfer ≤10 mg of conidia to 200 μl of TE buffer (10 mM Tris, 1 mM EDTA, pH 8.0). The suspension was boiled at 105° in a heat block for 12 min, incubated on ice for 2 min, then vortexed for 5 sec. Insoluble material was pelleted at 15,000 × *g* for 10 min at room temperature, after which 25 μl of supernatant was transferred to a new vial and frozen at −20° for storage. In our hands, this method works well for the amplification of polymerase chain reaction (PCR) products shorter than 1 kb. Method three was used for the preparation of genomic DNA for high-throughput sequencing. Strains were cultured in 25 ml of liquid GYP at 28° for 48 hr. Mycelia were washed with water and DNA was extracted with the Zymo Research Fungal DNA Miniprep Kit.

PCR assays were performed with MidSci Bullseye Taq DNA Polymerase or New England Biolabs Phusion High-Fidelity DNA Polymerase.

### Genome sequencing

DNA libraries for MiSeq sequencing (Illumina) were constructed from 1 ng of genomic DNA using the Illumina Nextera XT DNA Library Preparation Kit. Sequencing was performed with MiSeq Reagent Kit Version 3. Adapters were removed and low-quality reads were trimmed with CLC Genomics Workbench (Version 8.0). The datasets were deposited in the National Center for Biotechnology Information's (NCBI) Sequence Read Archive (Leinonen *et al.* 2011). They can be obtained with the following accession numbers: SRR3271586 (Fv999-$Sk^K$), SRR3273544 (JP98.75-$Sk^K$), SRR3273545 (JP98.111-$Sk^K$), and SRR3273546 (JP98.118-$Sk^K$). The datasets are of high quality. For example, draft genomes were assembled with CLC Genomics Workbench and all assemblies had N50 values over 90 kb with coverage levels between 49- and 73-fold (Table 2).

### CAPS markers

Cleaved amplified polymorphic sequence (CAPS) markers (Konieczny and Ausubel 1993) were used to help refine the location of $Sk^K$ (Table 3). CAPS markers were identified by first aligning genome sequencing reads from strain Fv999-$Sk^K$ to the Fv149-$Sk^S$ reference genome (NCBI, ASM14955v1) with Bowtie 2 (Langmead and Salzberg 2012) and then visually scanning aligned reads with Tablet (Milne *et al.* 2010) for polymorphisms in GGCC sites. This four-base sequence is cleaved by the restriction endonuclease *Hae*III. Six CAPS markers on chromosome V were chosen for this study, along with one CAPS marker on each of chromosomes I, VII, and XI (Table 3). PCR primers for each CAPS marker were designed to amplify a short product (<500 bp) from both Fv999-$Sk^K$ and Fv149-$Sk^S$ sequences. The PCR primers used for amplification of each CAPS marker are described in Supplemental Material, Table S1.

The following protocol was used to analyze the segregation patterns of CAPS markers in each individual of the Fv999-$Sk^K$ × Fv149-$Sk^S$ mapping population. Genomic DNA was isolated from each progeny, CAPS markers were amplified by PCR, and PCR products were digested with *Hae*III. The digested products were then examined for Fv999-$Sk^K$ or Fv149-$Sk^S$ cleavage patterns by gel electrophoresis on 2% agarose-TAE (40 mM Tris, 20 mM acetic acid, and 1 mM EDTA) gels. The *Hae*III-based DNA digest patterns of each CAPS marker for Fv999-$Sk^K$ and Fv149-$Sk^S$ alleles are listed in Table S2.

### Single nucleotide polymorphisms (SNPs)

Reads from each MiSeq dataset were aligned to the reference genome of strain Fv149-$Sk^S$ with Bowtie 2 (Langmead and Salzberg 2012). SAMtools 1.3 and BCFtools 1.3 were then used to report SNPs in variant call format (VCF) (Li *et al.* 2009; Danecek *et al.* 2011). Only reads that aligned to a single region of Fv149-$Sk^S$ with <10

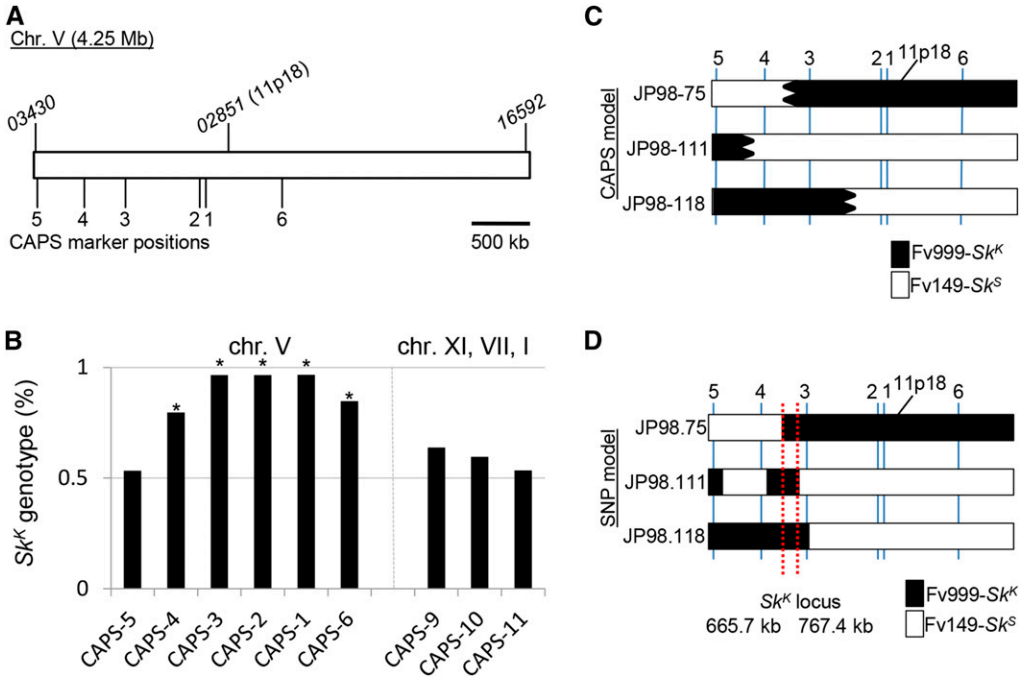


**Figure 2** F. *verticillioides Sk* is located within a 102 kb region of chromosome V. (A) A diagram of the 4.25 Mb sequence of chromosome V from Fv149-$Sk^S$ is shown. The annotated chromosome V sequence was downloaded from NCBI (CM000582.1). The positions of the first (*FVEG_03430*) and last (*FVEG_16592*) genes on the chromosome are indicated in the diagram. The approximate location of RFLP marker 11p18 is also shown. Marker 11p18 overlaps most of gene *FVEG_02851*. (B) A total of 60 progeny were isolated from a cross between Fv999-$Sk^K$ and Fv149-$Sk^S$. These progeny were genotyped with nine different CAPS markers. Markers CAPS-1 through CAPS-6 are located on chromosome V. Markers CAPS-9, CAPS-10, and CAPS-11 are found on chromosomes XI, VII, and I, respectively. Each bar represents the percentage of Fv999-$Sk^K$ genotypes recovered for each marker. An asterisk is placed above all markers whose recovery deviated significantly from a Mendelian ratio of 1:1 according to a $\chi^2$ test with $P < 0.01$. The biased transmission of Fv999-$Sk^K$ sequences was detected for all markers on chromosome V, except for CAPS-5. (C) The marker patterns for progeny JP98.75-$Sk^K$, JP98.111-$Sk^K$, and JP98.118-$Sk^K$ suggest that cross-over events occurred between CAPS-3 and CAPS-4 (for JP98.75-$Sk^K$), CAPS-4 and CAPS-5 (for JP98.111-$Sk^K$), and CAPS-2 and CAPS-3 (for JP98.118-$Sk^K$) (Table S3). These cross-overs did not identify an Fv999-$Sk^K$-derived region of chromosome V common to all three progeny. The predicted Fv999-$Sk^K$- and Fv149-$Sk^S$-inherited regions are shown in black and white, respectively. Irregular borders are used to indicate that exact cross-over positions could not be determined from the CAPS marker data. (D) SNP analysis was used to more accurately define cross-over positions for progeny JP98.75-$Sk^K$, JP98.111-$Sk^K$, and JP98.118-$Sk^K$. In addition to refining the location of the cross-overs identified by CAPS analysis, two additional cross-overs were identified between CAPS-3 and CAPS-4 on chromosome V of JP98.111-$Sk^K$. These findings helped delineate a single contiguous interval between position 665.7 kb and 767.4 kb on chromosome V as the only Fv999-$Sk^K$-derived chromosome V sequence common to all three progeny (red dotted lines). Therefore, this interval is referred to as the *Sk* region.

mismatches were used to produce the VCF files. Custom Perl scripts were then used to extract significant SNPs from the VCF files. Significant SNPs were defined as those which were supported by at least 90% of reads at each position. Only positions covered by more than nine reads were considered. Polymorphisms caused by insertions or deletions were ignored.

## Gene predictions

Protein-coding genes within the *Sk* region of Fv999-$Sk^K$ were predicted as follows: first, the sequence of the *Sk* region in Fv999-$Sk^K$ was obtained by *de novo* assembly of MiSeq reads (Table 2); second, the coding sequences of annotated genes from the *Sk* region of Fv149-$Sk^S$ were obtained from GenBank (CM000582.1); third, the Fv149-$Sk^S$ coding sequences were aligned to the *Sk* region of Fv999-$Sk^K$ with Clustal Omega (Sievers *et al.* 2011; Li *et al.* 2015); and fourth, the alignments were used to manually annotate protein-coding sequences within the Fv999-$Sk^K$ *Sk* region. These steps identified 41 putative protein-coding genes within the *Sk* region of Fv999-$Sk^K$. Augustus 3.2.1 (Stanke and Waack 2003) was then used for *de novo* prediction of protein-coding genes. Augustus predictions matched our manual annotation with the notable exception of an additional gene, *SKC1* (described below), within the *Sk* region of Fv999-$Sk^K$. The complete sequence and annotation of the 102 kb $Sk^K$ region from Fv999-$Sk^K$ can be downloaded from GenBank with accession number KU963213.

## Gene expression analysis

Sikhakolli *et al.* (2012) analyzed transcriptional changes in *F. verticillioides* during fruiting body development in Fv999-$Sk^K$ × Fv149-$Sk^S$ crosses by RNA sequencing (RNAseq) and deposited the datasets in NCBI's SRA database (Leinonen *et al.* 2011). The following datasets were downloaded from SRA: 2 hr post fertilization (hpf) (SRR1592416), 24 hpf (SRR1592417), 48 hpf (SRR1592418), 72 hpf (SRR1592419), 96 hpf (SRR1592420), and 144 hpf (SRR1592421). Reads were aligned to coding sequences of each predicted gene from the *Sk* region, plus flanking genes *FVEG_03199* and *FVEG_03163*, with Bowtie 2 (Langmead and Salzberg 2012). Reads per kilobase exon model per thousand mapped reads (RPKK), a variation upon RPKM as described by Mortazavi *et al.* (2008), were calculated for each coding sequence. Because of sequence differences between $Sk^K$-linked and $Sk^S$-linked alleles of genes in the *Sk* region, alignments and RPKK calculations were performed separately for $Sk^K$-linked and $Sk^S$-linked alleles. Thus, reported RPKK values are averages except for *SKC1*, which is only found in $Sk^K$ genotypes.

## Data availability

Data deposition: genome sequencing data are available through NCBI's Sequence Read Archive under accession numbers SRR3271586, SRR3273544, SRR3273545, and SRR3273546. Other sequence data are available from GenBank (KU963213).

## RESULTS

### Increased production of fruiting bodies by strain Fv999-$Sk^K$ on diluted CA

Directional crosses are often used to investigate sexual reproduction in heterothallic ascomycete fungi. In this type of cross, one parent is designated as the female and the other is designated as the male. The female provides protoperithecia, *i.e.*, immature fruiting bodies, which are fertilized by conidia from the male. After fertilization, protoperithecia develop into perithecia.

With *F. verticillioides*, CA is commonly used as a growth medium to study sexual processes. Its preparation essentially involves purchasing carrots from a local market, followed by peeling, blending, and autoclaving a predetermined weight of carrot within a specified volume of water (Leslie and Summerell 2006). Because we were curious about how the amount of carrot in CA influences the productivity of Fv999-$Sk^K$ × Fv149-$Sk^S$ crosses, Fv999-$Sk^K$ was cultured on 0.001×, 0.01×, 0.1×, 0.25×, 0.5×, and 1.0× CA, then fertilized with Fv149-$Sk^S$ conidia. Crosses performed on 0.1× and 0.25× CA resulted in three- to six-fold more perithecia than crosses performed on 0.5× and 1.0× CA (Figure 1). No perithecia were produced when crosses were performed on 0.001× and 0.01× CA (Figure 1). Additionally, less conidia were produced on 0.1× CA than on 0.25× CA (data not shown). Since conidia can be a source of cross-contamination, 0.1× CA was used as the crossing medium for the remainder of this study.

### RFLP 11p18 overlaps with FVEG_02851 on chromosome V

Although the sequence of RFLP1 was not available, we were able to obtain the sequence of RFLP 11p18 from the *Fusarium* Comparative Database. We used this sequence as the query in a Basic Local Alignment Search Tool (BLAST) (Altschul *et al.* 1990) search of the *F. verticillioides* reference genome. This search identified positions 1,672,753 to 1,673,602 on chromosome V (CM000582.1) as a match to 11p18. This region overlaps with most of the predicted coding sequence of gene *FVEG_02851* , which spans positions 1,672,886 to 1,673,739 and encodes a protein of unknown function. This position on chromosome V was used as a reference point to design CAPS markers near the *Sk* locus (Figure 2A).

### Loci linked to $Sk^K$ drive through meiosis

To begin refining the location of $Sk^K$ on chromosome V, Fv999-$Sk^K$ was crossed with Fv149-$Sk^S$ and the segregation patterns of nine CAPS markers were examined in 60 progeny. Both Fv999-$Sk^K$ and Fv149-$Sk^S$ patterns were inherited in a 1:1 ratio for chromosomes XI, VII, and I (Figure 2B and Table S3). In contrast, Fv999-$Sk^K$ patterns of CAPS markers on chromosome V were inherited more frequently than expected (≥79.6%; Figure 2B and Table S3). The only exception was CAPS-5, which is located ~20 kb from a telomere (Figure 2A and Table 3). Overall, these results mark the first independent confirmation of Xu and Leslie's (1996) original findings on the biased recovery of molecular markers linked to $Sk^K$ in $Sk^K$ × $Sk^S$ crosses.

### Genome sequencing refines Sk to a 102 kb region of chromosome V

To delineate the position of $Sk^K$ on chromosome V, we narrowed our focus to progeny JP98.75-$Sk^K$, JP98.111-$Sk^K$, and JP98.118-$Sk^K$. Even though CAPS marker analysis failed to identify an Fv999-$Sk^K$ region of chromosome V that was inherited by all three of these progeny (Figure 2C, black shaded regions), all were determined to carry the $Sk^K$ allele by phenotypic analysis (Figure 3 and data not shown). Therefore, their genomes were sequenced (Table 2) and their SNPs along chromosome V were examined. This analysis allowed us to identify two additional recombination events. Both of these recombination events occurred between CAPS-3 and CAPS-4 in the ascus that produced progeny JP98.111-$Sk^K$ (Figure 2D), explaining why they were not identified by our CAPS marker analysis. More importantly, the SNP profiles of all three progeny require that $Sk^K$ be located between positions 665,669 and 767,411 (Figure 2D, red lines) with respect to the reference sequence (GenBank, CM000582.1). We refer to this 102-kb contiguous sequence as the *Sk* region (GenBank, KU963213).

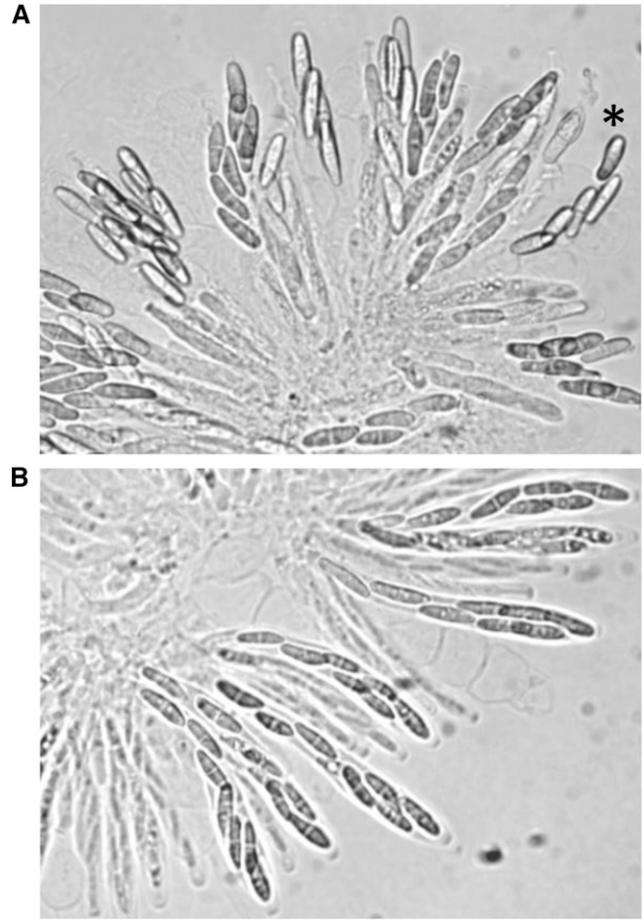


**Figure 3** Representative images of spore killing and resistance to spore killing in *F. verticillioides* asci. (A) Asci from a cross of progeny JP98.111-$Sk^K$ with Fv149-$Sk^S$. Only four ascospores are detected in most of the mature asci, confirming that JP98.111-$Sk^K$ carries the $Sk^K$ allele. The asterisk denotes an ascus where there appears to be five ascospores. Two possible explanations are that this 5th ascospore escaped killing, or it strayed from another ascus during the dissection and imaging process. (B) Asci from a cross of progeny JP98.111-$Sk^K$ with BM43.31-$Sk^K$. Eight ascospores can be detected in most of the mature asci, again confirming that progeny JP98.111-$Sk^K$ carries the $Sk^K$ allele.

### $Sk^K$ strains carry a unique gene in the Sk region

The *Sk* region spans 102,256 bases in Fv999-$Sk^K$, but only 101,743 bases in Fv149-$Sk^S$. A Clustal W-based alignment (Thompson *et al.* 1994) of the sequences from both strains is 102,557 bases long, with 301 gaps in the Fv999-$Sk^K$ sequence and 814 gaps in the Fv149-$Sk^S$ sequence (Figure 4). To identify specific regions in $Sk^K$ and $Sk^S$ strains with high levels of SNPs or gaps, the number of SNPs or gaps were calculated for each

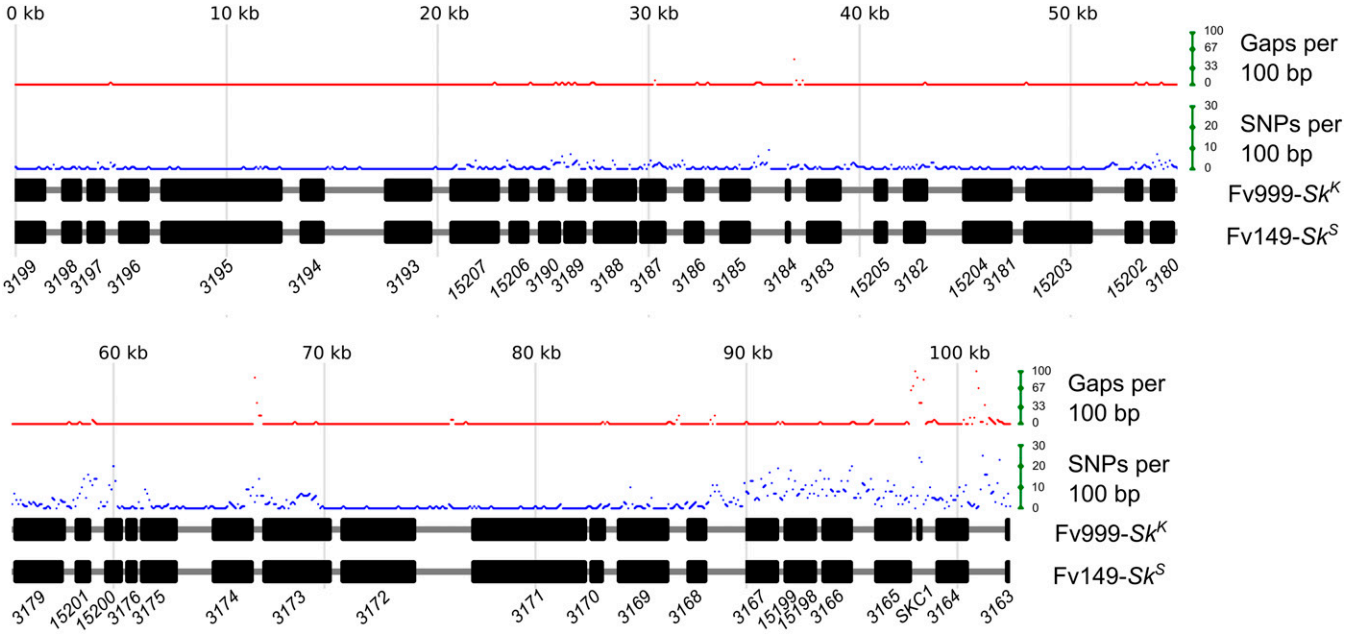


**Figure 4** Strain Fv999-*Sk*$^K$ carries a unique gene within a hyper-variable region of the *Sk* region. The *Sk* regions from Fv999-*Sk*$^K$ (GenBank, KU963213) and Fv149-*Sk*$^S$ (GenBank, CM000582.1, positions 665,669 to 767,411) were imported into BioEdit (Version 7.2.5) (Hall 1999) and aligned with Clustal W. Custom Perl scripts were used to examine base mismatches and gap positions, and to generate the diagram. The total number of mismatches (SNPs) between the two sequences was calculated for each 100-base nonoverlapping window of the alignment. The total number of gaps was also calculated for each 100-base nonoverlapping window. A gap position was not considered an SNP. By this definition, a window with 100 gaps cannot have SNPs. Black rectangles represent the coding regions of predicted genes. Gene names have been abbreviated according to their identification tags in the Fv149-*Sk*$^S$ annotation. For example: *FVEG_03199* was shortened to *3199*. A striking feature of the alignment is the presence of three hyper-variable intervals; spanning *FVEG_03180* to *FVEG_03175* , *FVEG_03174* to *FVEG_03173* , and *FVEG_03167* to the right border of the *Sk* region. A second striking feature is the presence of a unique gene, *SKC1*, in Fv999-*Sk*$^K$ only.

100-base window across the alignment. A qualitative analysis of these results finds at least three hyper-variable intervals (Figure 4). One of the short hyper-variable intervals spans genes *FVEG_03180* to *FVEG_03175* , while another spans genes *FVEG_03174* and *FVEG_03173* (Figure 4). The longest hyper-variable interval is ~14 kb long, spans gene *FVEG_03167* , and extends to the right border of the *Sk* region (Figure 4).

The *Sk* region in strain Fv149-*Sk*$^S$ includes 41 putative protein-coding genes (Figure 4 and Table 4). The *Sk* region in Fv999-*Sk*$^K$ carries the same 41 genes as well as one additional protein-coding gene, *SKC1* (for *Spore Killer Candidate 1*), which is located between *FVEG_03165* and *FVEG_03164* (Figure 4). A BLASTP search (Altschul *et al.* 1997) of the NCBI nonredundant protein database with the predicted 70 amino acid sequence of Skc1 identified hypothetical proteins with Expect values ranging from $2 \times 10^{-49}$ to $8 \times 10^{-04}$ from various *formae speciales* of the *F. oxysporum* species complex (Figure S1). No significant hits were identified in other species. A search of the NCBI Conserved Domain Database (Marchler-Bauer *et al.* 2010) failed to identify a domain within Skc1.

To confirm that *SKC1* is absent in Fv149-*Sk*$^S$, the sequences corresponding to the *FVEG_03165* -*FVEG_03164* intergenic region from Fv999-*Sk*$^K$ and Fv149-*Sk*$^S$ were aligned and examined. This intergenic region consists of 1234 and 755 bases in Fv999-*Sk*$^K$ and Fv149-*Sk*$^S$ respectively (Figure S2). The alignment revealed that this difference in length was due to the presence of *SKC1* in Fv999-*Sk*$^K$ and its absence from Fv149-*Sk*$^S$ (Figure S2). To confirm that the absence of *SKC1* in Fv149-*Sk*$^S$ was not due to an error in the reference genome sequence, we examined the lengths of the *FVEG_03165* -*FVEG_03164* intergenic region in our laboratory stocks of Fv999-SkK and Fv149-SkS by PCR. The PCR product lengths were consistent with the presence of *SKC1* in Fv999-*Sk*$^K$ and its absence from Fv149-*Sk*$^S$ (Figure 5).

Clustal W alignments were used to investigate the level of polymorphism between proteins encoded by the *Sk* region in Fv999-*Sk*$^K$ and Fv149-*Sk*$^S$ strains (Table 4). Analysis of these pairwise alignments revealed that Fveg_15199 is the most polymorphic protein of the region. Only 80% of the 133 amino acids of Fveg_15199 are identical between the two strains. This is a remarkably high level of polymorphism given that 34 of 41 proteins within the *Sk* region of Fv999-*Sk*$^K$ and Fv149-*Sk*$^S$ are >94% identical, and 40 of 41 are >88% identical (Table 4). A BLAST search of the NCBI nonredundant protein database identified homologs of Fveg_15199 in several *Fusarium*, *Neonectria*, *Scedosporium*, and *Aspergillus* species (Figure S3). A search of the NCBI Conserved Domain Database failed to identify a domain within Fveg_15199.

To shed light upon the transcriptional profile of protein-coding genes within the *Sk* region, we analyzed five *F. verticillioides* RNAseq datasets from NCBI's Sequence Read Archive. These datasets were for five time points following the induction of sexual development in a cross of Fv999-*Sk*$^K$ × Fv149-*Sk*$^S$ (Sikhakolli *et al.* 2012). Of the genes within the *Sk* region, *FVEG_03171* exhibited the greatest increase in expression from the first time point to the last time point (Table 5, 2.95 and 94.58 RPKK), suggesting that this gene may have an important role during later stages of sexual development. The corresponding protein, Fveg_03171 , includes a WSC-domain (pfam01822), which has been linked to carbohydrate-binding, cell wall integrity, and stress response. The gene *FVEG_03194* exhibited the greatest fold change when comparing differences between all five time points (>1050×) (Table 5). The Fveg_03194 protein does not contain recognized domains, although putative homologs can be found in *Fusarium*, *Nectria*, *Acremonium*, and *Trichoderma* fungi (Figure S4). Interestingly, *SKC1* reached the highest level of expression of all examined genes 2 hr after fertilization

**Table 4 Comparison of predicted protein sequences within the *Sk* region of Fv999-*Sk*$^K$ and Fv149-*Sk*$^S$**

| Name | Fv999-*Sk*$^K$ Length | Fv149-*Sk*$^S$ Length | Alignment Length | Identity (%) | Similarity (%) |
|---|---|---|---|---|---|
| 3198 | 279 | 279 | 279 | 99 | 99 |
| 3197 | 224 | 224 | 224 | 99 | 99 |
| 3196 | 462 | 462 | 462 | 100 | 100 |
| 3195 | 1786 | 1786 | 1786 | 100 | 100 |
| 3194 | 359 | 359 | 359 | 100 | 100 |
| 3193 | 655 | 655 | 655 | 100 | 100 |
| 15207 | 634 | 666 | 692 | 93 | 94 |
| 15206 | 274 | 274 | 274 | 100 | 100 |
| 3190 | 146 | 242 | 242 | 99 | 100 |
| 3189 | 246 | 336 | 336 | 89 | 91 |
| 3188 | 599 | 599 | 599 | 99 | 100 |
| 3187 | 327 | 327 | 327 | 98 | 99 |
| 3186 | 234 | 234 | 234 | 100 | 100 |
| 3185 | 409 | 409 | 409 | 100 | 100 |
| 3184 | 65 | 46 | 65 | 96 | 98 |
| 3183 | 513 | 513 | 513 | 100 | 100 |
| 15205 | 174 | 174 | 174 | 99 | 100 |
| 3182 | 379 | 355 | 379 | 97 | 98 |
| 15204 | 88 | 88 | 88 | 100 | 100 |
| 3181 | 667 | 667 | 667 | 100 | 100 |
| 15203 | 1029 | 1085 | 1085 | 99 | 99 |
| 15202 | 194 | 194 | 194 | 100 | 100 |
| 3180 | 359 | 359 | 359 | 97 | 99 |
| 3179 | 784 | 736 | 784 | 97 | 97 |
| 15201 | 227 | 227 | 227 | 89 | 90 |
| 15200 | 288 | 288 | 288 | 93 | 98 |
| 3176 | 139 | 139 | 139 | 100 | 100 |
| 3175 | 496 | 496 | 496 | 99 | 100 |
| 3174 | 620 | 620 | 620 | 96 | 97 |
| 3173 | 964 | 964 | 964 | 97 | 98 |
| 3172 | 1018 | 1018 | 1018 | 100 | 100 |
| 3171 | 1724 | 1724 | 1724 | 100 | 100 |
| 3170 | 230 | 212 | 230 | 98 | 98 |
| 3169 | 716 | 716 | 716 | 99 | 99 |
| 3168 | 299 | 299 | 299 | 100 | 100 |
| 3167 | 460 | 460 | 460 | 97 | 98 |
| 15199 | 133 | 133 | 133 | 80 | 86 |
| 15198 | 323 | 319 | 323 | 93 | 95 |
| 3166 | 466 | 466 | 466 | 90 | 95 |
| 3165 | 532 | 531 | 532 | 98 | 99 |
| Skc1 | 70 | Missing | na | na | na |
| 3164 | 476 | 479 | 479 | 98 | 99 |

The sequences of predicted proteins within the *Sk* region of Fv999-*Sk*$^K$ and Fv149-*Sk*$^S$ were imported into Bioedit 7.2.5 (Hall 1999) and aligned with Clustal W (Thompson *et al.* 1994). Sequence alignments were then analyzed for percent identity and percent similarity. Gapped-positions were excluded from the identity and similarity calculations. na, not applicable.

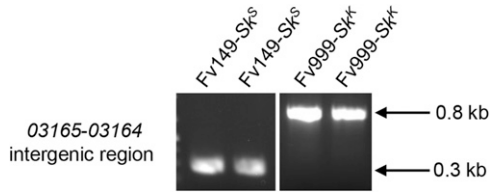


**Figure 5** The *Sk* region in Fv149-*Sk*$^S$ is missing *SKC1*. To confirm that *SKC1* is missing from the *Sk* region in Fv149-*Sk*$^S$, genomic DNA was isolated from two liquid cultures of Fv149-*Sk*$^S$ and two liquid cultures of Fv999-*Sk*$^K$. All four genomic DNA samples were used as templates in standard PCR reactions with the following oligonucleotide primers: 5′ CGAATGACCTGGGGAGCCATAA 3′ and 5′ TCTCTCCAC CACCTCCATCAGC 3′, which amplify the *FVEG_03165* -*FVEG_03164* intergenic regions from both Fv999-*Sk*$^K$ and Fv149-*Sk*$^S$. PCR products were visualized by ethidium bromide staining after electrophoresis through a 1% agarose-TAE gel. We observed PCR products with lengths that were consistent with absence of *SKC1* from Fv149-*Sk*$^S$ (287 bp) and presence of *SKC1* in Fv999-*Sk*$^K$ (767 bp).

(Table 5). *SKC1* transcript levels were also second only to *FVEG_03197* at the last time point (144 hr, Table 5). Fveg_03197 appears to be from a family of proteins widely conserved among bacteria and eukaryotes (Figure S5), but a function for it or its homologs is unknown.

## DISCUSSION

The segregation of alternate alleles into separate gametes during meiosis encourages genetic conflict (Burt and Trivers 2008). Evidence for this is found in meiotic drive, which occurs when an allele is transmitted through meiosis in a biased manner. Meiotic drive elements are found in a diverse range of fungi, where they achieve biased transmission through sexual reproduction by killing meiospores carrying an alternate allele (Turner and Perkins 1979; Kathariou and Spieth 1982; Raju 1994; Dalstra *et al.* 2003; Grognet *et al.* 2014). Therefore, fungal meiotic drive elements are often referred to as Spore killers. The molecular basis of meiotic drive by most Spore killers is unknown.

The existence of meiotic drive by spore killing in *Fusarium* was first recognized in 1982. More than three decades later, we still do not understand the molecular mechanism that mediates this process. This is similar to the situation in *Neurospora*, where three distinct Spore killers, namely *Sk-1*, *Sk-2*, and *Sk-3*, were identified in 1979 (Turner and Perkins 1979). A breakthrough in *Sk-2* research was recently made by refining the location of an *Sk-2* resistance gene to a 52 kb sequence of DNA (Hammond *et al.* 2012a). This provided the necessary foundation to clone and characterize this resistance gene (Hammond *et al.* 2012b), which in turn allowed for the isolation of killer-less *Sk-2* mutants (Harvey *et al.* 2014). Here, we have taken a similar approach toward identifying the genetic basis of *Sk*$^K$ in *F. verticillioides* by refining the position of *Sk*$^K$ to a 102 kb region of chromosome V.

As with previous work on *Sk*$^K$ (Xu and Leslie 1996), we observed a biased transmission of *Sk*$^K$-linked molecular markers (Figure 2B). This result was expected since the driving ability of *Sk*$^K$ should also affect the transmission of alleles linked to *Sk*$^K$. This phenomenon is referred to as genetic hitchhiking (Lyttle 1991). The closer a hitchhiker is to a meiotic driver, the more likely it is to be transmitted to the next generation through the sexual cycle. In our study, patterns of CAPS markers from the parent Fv999-*Sk*$^K$ were inherited at a higher frequency than could be attributed to chance alone for five of six markers on chromosome V, and the transmission bias generally decreased with increasing distance from the *Sk* region (Figure 2B). Surprisingly, CAPS-1 and CAPS-2 demonstrated higher levels of hitchhiking than CAPS-4 (Figure 2B), despite the latter being closer to the *Sk* region. One explanation for this could be the existence of a recombination hotspot between CAPS-4 and the *Sk* region; however, we do not have additional data to support this hypothesis.

While a recombination hotspot could explain the relatively low level of hitchhiking by CAPS-4, the opposite phenomenon of recombination-suppression is often associated with meiotic drive elements (reviewed by Lyttle 1991). For example, *Neurospora Sk-2* requires specific alleles of at least two genes to mediate drive, a resistance gene called *rsk* and a killer gene called *rfk* (Hammond *et al.* 2012b; Harvey *et al.* 2014). Each gene is located on a different arm of chromosome III (Harvey *et al.* 2014). For *Sk-2* to succeed as a meiotic driver, it is imperative that an *Sk-2* ascospore inherit both *rsk* and *rfk* alleles because separation can lead to

**Table 5 Expression analysis of genes from the *Sk* region during sexual development**

| ID | 2 h | 24 h | 48 h | 72 h | 96 h | 144 h | Min[a] | Max[b] | Fold Change[c] |
|---|---|---|---|---|---|---|---|---|---|
| *3198* | 39.17 | 150.92 | 38.40 | 24.98 | 28.10 | 20.10 | 20.10 | 150.92 | 7.51 |
| *3197* | 256.38 | 368.62 | 217.04 | 122.34 | 103.97 | 231.66 | 103.97 | 368.62 | 3.55 |
| *3196* | 0.83 | 0.13 | 0.87 | 0.56 | 0.83 | 0.87 | 0.13 | 0.87 | 6.59 |
| *3195* | 2.49 | 0.57 | 2.48 | 0.62 | 5.80 | 0.79 | 0.57 | 5.80 | 10.12 |
| *3194* | 0.25 | 0.12 | 0.30 | 14.02 | 124.53 | 1.20 | 0.12 | 124.53 | 1050.12 |
| *3193* | 138.42 | 94.82 | 71.69 | 43.35 | 80.19 | 75.41 | 43.35 | 138.42 | 3.19 |
| *15207* | 1.41 | 1.35 | 16.98 | 1.71 | 2.05 | 2.46 | 1.35 | 16.98 | 12.55 |
| *15206* | 0.78 | 1.40 | 5.23 | 1.29 | 0.76 | 1.08 | 0.76 | 5.23 | 6.86 |
| *3190* | 0.00 | 0.00 | 0.00 | 0.00 | 0.23 | 0.00 | 0.00 | 0.23 | 2.32 |
| *3189* | 0.00 | 0.00 | 0.00 | 0.05 | 0.50 | 0.00 | 0.00 | 0.50 | 4.95 |
| *3188* | 1.73 | 0.36 | 1.58 | 0.48 | 2.72 | 0.40 | 0.36 | 2.72 | 7.65 |
| *3187* | 1.90 | 0.97 | 1.34 | 31.36 | 42.16 | 0.71 | 0.71 | 42.16 | 59.47 |
| *3186* | 1.45 | 0.55 | 0.81 | 0.77 | 0.37 | 0.61 | 0.37 | 1.45 | 3.91 |
| *3185* | 5.41 | 3.74 | 6.17 | 2.61 | 1.72 | 1.51 | 1.51 | 6.17 | 4.09 |
| *3184* | 0.58 | 0.00 | 1.19 | 0.84 | 9.94 | 0.79 | 0.00 | 9.94 | 99.38 |
| *3183* | 59.62 | 22.63 | 32.99 | 13.12 | 29.15 | 21.10 | 13.12 | 59.62 | 4.54 |
| *15205* | 4.06 | 1.68 | 6.07 | 3.12 | 10.00 | 1.23 | 1.23 | 10.00 | 8.15 |
| *3182* | 0.30 | 0.00 | 1.19 | 0.00 | 0.29 | 0.00 | 0.00 | 1.19 | 11.93 |
| *15204* | 5.10 | 3.36 | 84.28 | 5.20 | 12.73 | 5.45 | 3.36 | 84.28 | 25.10 |
| *3181* | 2.16 | 0.50 | 5.24 | 0.50 | 1.93 | 0.66 | 0.50 | 5.24 | 10.57 |
| *15203* | 4.74 | 0.12 | 3.02 | 1.00 | 4.72 | 0.95 | 0.12 | 4.74 | 39.22 |
| *15202* | 1.05 | 0.44 | 8.61 | 7.61 | 9.45 | 0.74 | 0.44 | 9.45 | 21.57 |
| *3180* | 2.20 | 0.00 | 3.14 | 0.14 | 0.98 | 0.17 | 0.00 | 3.14 | 31.38 |
| *3179* | 1.28 | 0.06 | 1.14 | 0.10 | 2.70 | 0.09 | 0.06 | 2.70 | 47.85 |
| *15201* | 4.11 | 0.57 | 4.26 | 1.33 | 4.46 | 0.49 | 0.49 | 4.46 | 9.01 |
| *15200* | 1.02 | 0.55 | 0.32 | 0.36 | 0.29 | 0.24 | 0.24 | 1.02 | 4.16 |
| *3176* | 126.00 | 50.26 | 80.75 | 15.66 | 31.67 | 29.31 | 15.66 | 126.00 | 8.05 |
| *3175* | 48.87 | 12.93 | 38.03 | 9.13 | 19.60 | 13.41 | 9.13 | 48.87 | 5.35 |
| *3174* | 4.53 | 1.43 | 8.61 | 0.94 | 4.68 | 1.29 | 0.94 | 8.61 | 9.18 |
| *3173* | 1.04 | 0.17 | 2.86 | 0.42 | 1.90 | 0.42 | 0.17 | 2.86 | 17.29 |
| *3172* | 1.01 | 0.00 | 3.78 | 0.45 | 2.16 | 0.70 | 0.00 | 3.78 | 37.81 |
| *3171* | 2.95 | 37.34 | 38.55 | 117.07 | 44.37 | 94.58 | 2.95 | 117.07 | 39.66 |
| *3170* | 0.14 | 0.19 | 0.00 | 0.81 | 0.13 | 0.44 | 0.00 | 0.81 | 8.09 |
| *3169* | 5.48 | 0.61 | 5.38 | 3.02 | 7.40 | 2.61 | 0.61 | 7.40 | 12.05 |
| *3168* | 4.33 | 21.39 | 2.58 | 13.90 | 7.76 | 2.19 | 2.19 | 21.39 | 9.77 |
| *3167* | 0.17 | 0.71 | 0.13 | 0.21 | 0.12 | 0.04 | 0.04 | 0.71 | 19.47 |
| *15199* | 0.07 | 0.00 | 0.00 | 0.00 | 0.00 | 0.00 | 0.00 | 0.07 | 0.71 |
| *15198* | 1.34 | 0.12 | 0.56 | 0.21 | 0.31 | 0.19 | 0.12 | 1.34 | 11.68 |
| *3166* | 0.99 | 0.17 | 1.43 | 0.24 | 0.31 | 0.22 | 0.17 | 1.43 | 8.36 |
| *3165* | 20.77 | 11.51 | 13.49 | 9.68 | 8.41 | 4.09 | 4.09 | 20.77 | 5.07 |
| *SKC1* | 481.58 | 392.59 | 227.42 | 211.66 | 360.52 | 97.65 | 97.65 | 481.58 | 4.93 |
| *3164* | 16.11 | 30.78 | 16.09 | 6.78 | 16.48 | 15.70 | 6.78 | 30.78 | 4.54 |

[a] The minimum RPKK in the table.
[b] The maximum RPKK in the table.
[c] Fold change was calculated by dividing the maximum RPKK by the minimum RPKK. If the minimum RPKK for a gene was 0 it was arbitrarily assigned a minimum RPKK of 0.1 to approximate a fold change value. Unrounded maximum and minimum RPKK values (not shown) were used to calculate fold change values.

a self-killing genotype (Hammond *et al.* 2012b). This helps explain why *Sk-2* is associated with a 30 cM "recombination-blocked" interval of chromosome III (Campbell and Turner 1987; Harvey *et al.* 2014). By suppressing recombination between *rsk* and *rfk*, *Sk-2* can prevent these critical components of drive from separating during meiosis. With respect to *F. verticillioides* $Sk^K$, recombination-suppression, if it exists at all, does not appear to be a significant phenomenon. For example, our CAPS marker analysis identified 12 recombination events between CAPS-3 and CAPS-4 ($n = 59$, Table S3), and two recombination events between CAPS-2 and CAPS-3 ($n = 59$, Table S3). This relatively high number of recombination events near the *Sk* region argues against an *Sk-2*-like recombination block for $Sk^K$.

If *F. verticillioides* $Sk^K$ requires multiple genes to function as a meiotic drive element, all should be found within the 102 kb *Sk* region defined by this study. For example, SNP-profiling of progeny JP98.75-$Sk^K$, JP98.111-$Sk^K$, and JP98.118-$Sk^K$ indicates that only this region of chromosome V is common between these three progeny and their Fv999-$Sk^K$ parent (Figure 2D and Figure 4). Assuming killing is mediated by two or more distinct genes within the *Sk* region, the close proximity of these genes may negate the requirement for a *Neurospora Sk-2*-like recombination block. Alternatively, meiotic drive and spore killing may be mediated by a single gene. A precedent for this is seen in the *het-s* spore killing mechanism of *Podospora anserina* (Coustou *et al.* 1997; Saupe 2011). This system is controlled by two alternate alleles of a single gene, named *het-s* and *het-S*. The former allele, *het-s*, encodes the HET-s prion and is the meiotic driver, while the latter allele, *het-S*, encodes the HET-S protein. Interaction of the HET-s prion with the HET-S protein causes HET-S to relocate to cell membranes, resulting in cell death, presumably through loss of membrane integrity (Seuring *et al.* 2012). Ascospores with *het-s* genotypes escape cell death because

they do not produce the HET-S protein, thus the *het-s* prion is not toxic to them. This is just one example of how meiotic drive and spore killing can be mediated by alternate alleles of a single gene in fungi. Grognet *et al.* (2014) have recently identified *spok1* and *spok2*, two additional spore killing genes in *P. anserina*, both of which also appear to be single-gene-based meiotic drive systems.

In the current study, comparative sequence analysis revealed multiple differences between the 102 kb *Sk* region in $Sk^K$ and $Sk^S$ strains of *F. verticillioides*. Presumably, one or more of these differences is the genetic basis for the different *Sk* phenotypes exhibited by the strains. An analysis of SNPs and gaps identified at least three hyper-variable intervals within the *Sk* region (Figure 4). The interspersed nature of these intervals is somewhat surprising. The most striking difference, however, is the presence of the *SKC1* gene in $Sk^K$ strains. Differences between the hyper-variable intervals and *SKC1* in $Sk^K$ *vs.* $Sk^S$ strains raise at least two key questions: (1) are the hyper-variable intervals and/or *SKC1* responsible for killing, and (2) do they correspond to the $Sk^K$ allele that was previously defined by phenotypic analysis (Kathariou and Spieth 1982). The high level of expression of *SKC1* throughout sexual development is consistent with its involvement in sexual reproduction. However, in addition to *SKC1* and the hyper-variable intervals, there are less dramatic sequence differences between genes and intergenic sequences of the *Sk* region in $Sk^K$ and $Sk^S$ strains. The current data do not rule out the possibility that one or more of these differences is responsible for the $Sk^K$ and $Sk^S$ phenotypes. As a result, our efforts are now focused on targeted deletions of *SKC1* and other sequences within the *Sk* region to determine the genetic basis of the spore killing phenotype in *F. verticillioides*.

## ACKNOWLEDGMENTS

Dr. John Leslie (Kansas State University) and Dr. Frances Trail (Michigan State University) kindly donated strains Fv999-$Sk^K$ and Fv149-$Sk^S$. We thank the Fungal Genetics Stock Center (McCluskey *et al.* 2010) for other key strains and the Broad Institute of Harvard and the Massachusetts Institute of Technology (www.broad.mit.edu) for access to the *Fusarium* Comparative Database. Chris McGovern and Nathane Orwig of the National Center for Agricultural Utilization Research provided much appreciated technical assistance. We thank Dr. Sven Saupe (Université de Bordeaux) for sharing his knowledge of the *het-s* spore killing mechanism. T.M.H. was supported by a grant from the Eunice Kennedy Shriver National Institute of Child Health and Human Development (NICHD) of the National Institutes of Health (1R15HD076309-01). Mention of trade names or commercial products in this article is solely for the purpose of providing specific information and does not imply recommendation or endorsement by the US Department of Agriculture. The US Department of Agriculture is an equal opportunity provider and employer.

## LITERATURE CITED

Altschul, S. F., W. Gish, W. Miller, E. W. Myers, and D. J. Lipman, 1990 Basic local alignment search tool. J. Mol. Biol. 215: 403–410.

Altschul, S. F., T. L. Madden, A. A. Schäffer, J. Zhang, Z. Zhang *et al.*, 1997 Gapped BLAST and PSI-BLAST: a new generation of protein database search programs. Nucleic Acids Res. 25: 3389–3402.

Bacon, C. W., and D. M. Hinton, 1996 Symptomless endophytic colonization of maize by *Fusarium moniliforme*. Can. J. Bot. 74: 1195–1202.

Burt, A., and R. Trivers, 2008 *Genes in Conflict: The Biology of Selfish Genetic Elements*. Harvard University Press. Cambridge, MA.

Campbell, J. L., and B. C. Turner, 1987 Recombination block in the *Spore killer* region of *Neurospora*. Genome 29: 129–135.

Coustou, V., C. Deleu, S. Saupe, and J. Begueret, 1997 The protein product of the *het-s* heterokaryon incompatibility gene of the fungus *Podospora anserina* behaves as a prion analog. Proc. Natl. Acad. Sci. USA 94: 9773–9778.

Dalstra, H. J. P., K. Swart, A. J. M. Debets, S. J. Saupe, and R. F. Hoekstra, 2003 Sexual transmission of the [Het-S] prion leads to meiotic drive in *Podospora anserina*. Proc. Natl. Acad. Sci. USA 100: 6616–6621.

Danecek, P., A. Auton, G. Abecasis, C. A. Albers, E. Banks *et al.*, 2011 The variant call format and VCFtools. Bioinformatics 27: 2156–2158.

Gelderblom, W. C., K. Jaskiewicz, W. F. Marasas, P. G. Thiel, R. M. Horak *et al.*, 1988 Fumonisins – novel mycotoxins with cancer-promoting activity produced by *Fusarium moniliforme*. Appl. Environ. Microbiol. 54: 1806–1811.

Gelderblom, W. C., N. P. Kriek, W. F. Marasas, and P. G. Thiel, 1991 Toxicity and carcinogenicity of the *Fusarium moniliforme* metabolite, fumonisin B1, in rats. Carcinogenesis 12: 1247–1251.

Grognet, P., H. Lalucque, F. Malagnac, and P. Silar, 2014 Genes that bias Mendelian segregation. PLoS Genet. 10: e1004387.

Hall, T. A., 1999 BioEdit: a user-friendly biological sequence alignment editor and analysis program for Windows 95/98/NT. Nucleic Acids Symp. Ser. 41: 95–98.

Hammond, T. M., D. G. Rehard, B. C. Harris, and P. K. T. Shiu, 2012a Fine-scale mapping in *Neurospora crassa* by using genome-wide knockout strains. Mycologia 104: 321–323.

Hammond, T. M., D. G. Rehard, H. Xiao, and P. K. T. Shiu, 2012b Molecular dissection of the *Neurospora* Spore killer elements. Proc. Natl. Acad. Sci. USA 109: 12093–12098.

Harrison, L. R., B. M. Colvin, J. T. Greene, L. E. Newman, and J. R. Cole, Jr., 1990 Pulmonary edema and hydrothorax in swine produced by fumonisin B1, a toxic metabolite of *Fusarium moniliforme*. J. Vet. Diagn. Invest. 2: 217–221.

Harvey, A. M., D. G. Rehard, K. M. Groskreutz, D. R. Kuntz, K. J. Sharp *et al.*, 2014 A critical component of meiotic drive in *Neurospora* is located near a chromosome rearrangement. Genetics 197: 1165–1174.

Henderson, S. T., G. A. Eariss, and D. Catcheside, 2005 Reliable PCR amplification from *Neurospora crassa* genomic DNA obtained from conidia. Fungal Genet. Newsl. 52: 24.

Kathariou, S., and P. T. Spieth, 1982 Spore killer polymorphism in *Fusarium moniliforme*. Genetics 102: 19–24.

Kellerman, T. S., W. F. Marasas, J. G. Pienaar, and T. W. Naudé, 1972 A mycotoxicosis of equidae caused by *Fusarium moniliforme* sheldon. A preliminary communication. Onderstepoort J. Vet. Res. 39: 205–208.

Kellerman, T. S., W. F. Marasas, P. G. Thiel, W. C. Gelderblom, M. Cawood *et al.*, 1990 Leukoencephalomalacia in two horses induced by oral dosing of fumonisin B1. Onderstepoort J. Vet. Res. 57: 269–275.

Klittich, C., and J. F. Leslie, 1988 Nitrate reduction mutants of *Fusarium moniliforme* (*Gibberella fujikuroi*). Genetics 118: 417–423.

Konieczny, A., and F. M. Ausubel, 1993 A procedure for mapping *Arabidopsis* mutations using co-dominant ecotype-specific PCR-based markers. Plant J. 4: 403–410.

Langmead, B., and S. L. Salzberg, 2012 Fast gapped-read alignment with Bowtie 2. Nat. Methods 9: 357–359.

Leinonen, R., H. Sugawara, and M. Shumway, 2011 The sequence read archive. Nucleic Acids Res. 39: D19–D21.

Leslie, J. F., and B. A. Summerell, 2006 *The Fusarium Laboratory Manual*. Blackwell Publishing, Ames, IA.

Li, H., B. Handsaker, A. Wysoker, T. Fennell, J. Ruan *et al.*, 2009 The Sequence Alignment/Map format and SAMtools. Bioinformatics 25: 2078–2079.

Li, W., A. Cowley, M. Uludag, T. Gur, H. McWilliam *et al.*, 2015 The EMBL-EBI bioinformatics web and programmatic tools framework. Nucleic Acids Res. 43: W580–584.

Lyttle, T. W., 1991 Segregation distorters. Annu. Rev. Genet. 25: 511–557.

Ma, L. J., H. C. van der Does, K. A. Borkovich, J. J. Coleman, M. J. Daboussi *et al.*, 2010 Comparative genomics reveals mobile pathogenicity chromosomes in *Fusarium*. Nature 464: 367–373.

Marasas, W. F. O., 2001 Discovery and occurrence of the fumonisins: a historical perspective. Environ. Health Perspect. 109(Suppl 2): 239–243.

Marasas, W. F., T. S. Kellerman, W. C. Gelderblom, J. A. Coetzer, P. G. Thiel *et al.*, 1988 Leukoencephalomalacia in a horse induced by fumonisin B1 isolated from *Fusarium moniliforme*. Onderstepoort J. Vet. Res. 55: 197–203.

Marchler-Bauer, A., S. Lu, J. B. Anderson, F. Chitsaz, M. K. Derbyshire *et al.*, 2010 CDD: a Conserved Domain Database for the functional annotation of proteins. Nucleic Acids Res. 39: D225–D229.

Martin, S. H., B. D. Wingfield, M. J. Wingfield, and E. T. Steenkamp, 2011 Structure and evolution of the *Fusarium* mating type locus: new insights from the *Gibberella fujikuroi* complex. Fungal Genet. Biol. 48: 731–740.

McCluskey, K., A. Wiest, and M. Plamann, 2010 The Fungal Genetics Stock Center: a repository for 50 years of fungal genetics research. J. Biosci. 35: 119–126.

Milne, I., M. Bayer, L. Cardle, P. Shaw, G. Stephen *et al.*, 2010 Tablet – next generation sequence assembly visualization. Bioinformatics 26: 401–402.

Missmer, S. A., L. Suarez, M. Felkner, E. Wang, A. H. Merrill, Jr *et al.*, 2006 Exposure to fumonisins and the occurrence of neural tube defects along the Texas-Mexico border. Environ. Health Perspect. 114: 237–241.

Mortazavi, A., B. A. Williams, K. McCue, L. Schaeffer, and B. Wold, 2008 Mapping and quantifying mammalian transcriptomes by RNA-Seq. Nat. Methods 5: 621–628.

Munkvold, G. P., 2003 Epidemiology of *Fusarium* diseases and their mycotoxins in maize ears. Eur. J. Plant Pathol. 109: 705–713.

Munkvold, G. P., and A. E. Desjardins, 1997 Fumonisins in maize: can we reduce their occurrence? Plant Dis. 81: 556–565.

Raju, N. B., 1994 Ascomycete spore killers: Chromosomal elements that distort genetic ratios among the products of meiosis. Mycologia 86: 461–473.

Reynoso, M. M., S. N. Chulze, K. A. Zeller, A. M. Torres, and J. F. Leslie, 2009 Genetic structure of *Fusarium verticillioides* populations isolated from maize in Argentina. Eur. J. Plant Pathol. 123: 207–215.

Saupe, S. J., 2011 The [Het-s] prion of *Podospora anserina* and its role in heterokaryon incompatibility. Semin. Cell Dev. Biol. 22: 460–468.

Seuring, C., J. Greenwald, C. Wasmer, R. Wepf, S. J. Saupe *et al.*, 2012 The mechanism of toxicity in HET-S/HET-s prion incompatibility. PLoS Biol. 10: e1001451.

Sidhu, G. S., 1984 Genetics of *Gibberella fujikuroi* V. *Spore killer* alleles in *G. fujikuroi*. J. Hered. 75: 237–238.

Sievers, F., A. Wilm, D. Dineen, T. J. Gibson, K. Karplus *et al.*, 2011 Fast, scalable generation of high-quality protein multiple sequence alignments using Clustal Omega. Mol. Syst. Biol. 7: 539.

Sikhakolli, U. R., F. López-Giráldez, N. Li, R. Common, J. P. Townsend *et al.*, 2012 Transcriptome analyses during fruiting body formation in *Fusarium graminearum* and *Fusarium verticillioides* reflect species life history and ecology. Fungal Genet. Biol. 49: 663–673.

Stanke, M., and S. Waack, 2003 Gene prediction with a hidden Markov model and a new intron submodel. Bioinformatics 19(Suppl 2): 215–225.

Thompson, J. D., D. G. Higgins, and T. J. Gibson, 1994 CLUSTAL W: improving the sensitivity of progressive multiple sequence alignment through sequence weighting, position-specific gap penalties and weight matrix choice. Nucleic Acids Res. 22: 4673–4680.

Tuite, J., 1969 *Plant Pathological Methods: Fungi and Bacteria*. Burgess Publishing Company, Minneapolis.

Turner, B. C., and D. D. Perkins, 1979 *Spore killer*, a chromosomal factor in *Neurospora* that kills meiotic products not containing it. Genetics 93: 587–606.

Vogel, H. J., 1956 A convenient growth medium for *Neurospora* (Medium N). Microb. Genet Bull 13: 42–43.

White, D. G., 1998 *Compendium of Corn Diseases*. APS Press, St. Paul, MN.

Wu, F., 2007 Measuring the economic impacts of *Fusarium* toxins in animal feeds. Anim. Feed Sci. Technol. 137: 363–374.

Xu, J. R., and J. F. Leslie, 1996 A genetic map of *Gibberella fujikuroi* mating population A (*Fusarium moniliforme*). Genetics 143: 175–189.

Xu, J. R., K. Yan, M. B. Dickman, and J. F. Leslie, 1995 Electrophoretic karyotypes distinguish the biological species of *Gibberella fujikuroi* (*Fusarium* Section Liseola). Mol. Plant Microbe Interact. 8: 74–84.

*Communicating editor: K. Dawe*